

## EFFECT OF RARE-EARTH ELEMENT DOPING ON FE–GA ALLOYS PROPERTIES: *AB INITIO* AND MONTE CARLO MODELLING

*M.V. Matyunina*<sup>1</sup>, *A.S. Sokol*<sup>1</sup>, *O.O. Pavlakhina*<sup>1</sup>, *M.A. Zagrebin*<sup>1</sup>,  
*V.V. Sokolovskiy*<sup>1</sup>, *V.D. Buchelnikov*<sup>1</sup>

<sup>1</sup>Chelyabinsk State University, Chelyabinsk, Russian Federation

E-mail: matunins.fam@mail.ru, sokolanna687@mail.ru, pavluhinaoo@mail.ru,  
miczag@mail.ru, vsokolovsky84@mail.ru, buche@csu.ru

In this paper, we study the effect of a small addition of rare earth elements on the structural, magnetic, and magnetomechanical properties of  $\text{Fe}_{80,47}\text{Ga}_{18,75}\text{RE}_{0,78}$  alloys (RE = Tb, Pr, Er) in the  $\text{D0}_3$  phase using the density functional theory and the Monte Carlo method. Geometrical optimization of the crystal lattice performed on a 128-atom supercell showed that one RE substitution atom leads to an increase in the volume per atom of the cell by  $\approx 1\%$ . It is shown that  $\text{Fe}_{80,47}\text{Ga}_{18,75}\text{RE}_{0,78}$  alloys are mechanically stable, however a significant decrease in  $C'$  is observed. The addition of RE atoms has a significant effect on the magnetic anisotropy of the alloy and changes the direction of the easy axis from  $[001]$  to  $[111]$  compared to  $\text{Fe}_{81,25}\text{Ga}_{18,75}$ . The highest value of tetragonal magnetostriction  $\lambda_{001} \approx -179 \times 10^{-6}$  is found in the  $\text{Fe}_{80,47}\text{Ga}_{18,75}\text{Tb}_{0,78}$  alloy. The calculated value of the Curie temperature in compositions containing RE is  $\approx 200$  K lower than that of  $\text{Fe}_{81,25}\text{Ga}_{18,75}$ , and the lowest value is found in the  $\text{Fe}_{80,47}\text{Ga}_{18,75}\text{Er}_{0,78}$  alloy. This behavior is due to the presence of antiferromagnetic exchange interactions between Er and Fe atoms in the first and second coordination spheres.

*Keywords:* magnetostriction; Fe-Ga alloys; density functional theory; rare earth elements.

## Introduction

Magnetostrictive materials are an important part of modern manufacturing technologies. Due to their volume-preserving deformation in the direction of the applied magnetic field, they are widely used in actuators, sensors and transducers. The elongation of the sample under a magnetic field or mechanical stress is a consequence of magnetoelastic coupling arising mainly from spin-orbit interaction associated with elastic distortions. The highest value of saturation magnetostriction  $3/2\lambda_s = 2630 \times 10^{-6}$  at room temperature was found in the Tb-Fe<sub>2</sub> alloy [1]. However, this alloy, like the DyFe<sub>2</sub> alloy ( $3/2\lambda_s = 650 \times 10^{-6}$ ), has large magnetocrystalline anisotropy (MA), which requires strong magnetic fields to bring it to saturation. To reduce MA, Tb and Dy were added to Fe in the correct proportion, and the resulting intermetallic compound Tb<sub>0,27</sub>Dy<sub>0,73</sub>Fe<sub>2</sub> (commercially known as Terfenol-D) [2] showed  $3/2\lambda_s = 2000 \times 10^{-6}$  at room temperature. One of the drawbacks of Terfenol-D is its brittleness, which limits its ability to withstand shock loads or operate in tension.

The observed high magnetostriction values of  $350 \times 10^{-6}$  in magnetic fields of  $\approx 100$  Oe in Fe<sub>83</sub>Ga<sub>17</sub> and Fe<sub>81</sub>Ga<sub>19</sub> alloys [3–6] have contributed to a new stage in the study of magnetostrictive materials. In contrast to Tb<sub>0,27</sub>Dy<sub>0,73</sub>Fe<sub>2</sub>, Fe–Ga alloys have high tensile strength ( $\sim 500$  MPa), weak temperature dependence of magnetomechanical properties ( $-20^\circ\text{C}$  to  $80^\circ\text{C}$ ), are inexpensive and corrosion resistant. Moreover,  $3/2\lambda_s$  reaches two positive peaks around 19 at.% Ga ( $380 \times 10^{-6}$  for quenched alloys) and

27 at.% Ga ( $440 \times 10^{-6}$  for quenched alloys) [7]. Studies of  $\text{Fe}_{100-x}\text{Ga}_x$  binary alloys over the last 2 decades have revealed the dependence of  $3/2\lambda_s$  on Ga concentration, elastic properties, and formation of phase composition depending on production and quenching technology [7–12]. In particular, the region of the first magnetostriction peak is associated with the disordered A2 body centered cubic (bcc) structure. The metastable phase diagram of  $\text{Fe}_{85-65}\text{Ga}_{15-35}$  [7, 8] alloys constructed on the basis of the investigations determines the boundaries of the A2/(A2+D0<sub>3</sub>) and (A2+D0<sub>3</sub>)/D0<sub>3</sub> regions and their dependence on the technological process. The boundary of the single-phase A2 region extends up to 17,6 at.% Ga in slowly cooled samples and up to 20.6 at.% Ga in quenched samples depending on the time and temperature of subsequent isothermal annealing. The beginning of the D0<sub>3</sub> phase boundary varies from 22,1 at.% to 23,4 at.%, which, in turn, affects the width of the (A2+D0<sub>3</sub>) region. Similar studies carried out by X-ray diffraction methods [13, 14] of similar compositions  $\text{Fe}_{80,5}\text{Ga}_{19,5}$  and  $\text{Fe}_{80}\text{Ga}_{20}$  detected two phases in slowly cooled samples (67% A2 + 33% D0<sub>3</sub>) and (30% A2 + 70% D0<sub>3</sub>), respectively, whereas in quenched samples only the A2 structure was observed.

Initially, the version of the origin of MA proposed by Clark et al. [15] was that short-range ordered Ga pairs form clusters that act as locally distorted anisotropic defects cause strain of  $\alpha$ -Fe lattice along the [100] directions under application of magnetic or stress fields. Later, several inclusions of the D0<sub>3</sub> phase structure with a scale of  $< 2$  nm in the A2 cubic matrix were found in  $\text{Fe}_{81}\text{Ga}_{19}$  alloys using high-resolution transmission electron microscopy [16–21]. These D0<sub>3</sub> nanoprecipitates can be transformed into the body-centered tetragonal (bct) phase D0<sub>22</sub> (L6<sub>0</sub>) via diffusionless lattice rearrangement under the action of Bain stresses and, as a consequence, cause local deformation of the surrounding matrix, which leads to high magnetostriction values.

To enhance the tetragonal magnetostriction, binary  $\text{Fe}_{83-81}\text{Ga}_{17-19}$  systems were doped with rare earth (RE) elements [22–28]. RE atoms have strong local magnetocrystalline anisotropy due to the large spin-orbit coupling and the highly anisotropic localized nature of the  $4f$  electron charge distribution. Together with the large atomic radius compared to Fe and Ga atoms, this can lead to a local deformation effect in the FeGa lattice due to the inclusion of the RE element and, as a consequence, higher magnetostriction values. Focusing on Tb-doped Fe–Ga alloys, Jiang et al. reported an increase in magnetostriction from 72 to  $160 \times 10^{-6}$  in directionally solidified  $\text{Fe}_{83}\text{Ga}_{17}\text{Tb}_x$  ( $x = 0, 2$ ) [23] polycrystalline alloys. Using three methods (casting, melt-quenching and melt-spinning) to produce Tb-doped alloys  $(\text{Fe}_{0,83}\text{Ga}_{0,17})_{100-x}\text{Tb}_x$  ( $x = 0 - 0, 47$ ), Wu et al. [22] showed that the solid solubility of Tb atoms in A2 matrix increases with increasing the cooling rate. Magnetostriction is greatly improved when solid Tb is dissolved in  $\text{Fe}_{83}\text{Ga}_{17}$  alloys, and giant values of perpendicular magnetostriction up to  $-886 \times 10^{-6}$  were achieved in  $(\text{Fe}_{0,83}\text{Ga}_{0,17})_{99,77}\text{Tb}_{0,23}$  ribbons prepared by spinning from the melt. The data obtained in the experimental work [26] reflect the effect of Er addition on the microstructure and magnetic and microstructural properties of  $\text{Fe}_{83}\text{Ga}_{17}\text{Er}_x$  ( $0 < x < 1, 2$ ). It was shown that the optimal addition of Er  $x = 0, 6$  at.% increases the magnetostriction value up to 170 ppm in the [110]-textured polycrystalline  $\text{Fe}_{83}\text{Ga}_{17}\text{Er}_{0,6}$  sample, which is  $\approx 275\%$  higher than that of the corresponding parent  $\text{Fe}_{83}\text{Ga}_{17}$  compound. Based on experimental and computational studies conducted by He et al. [24], it is surmised that the giant magnetostriction in rare-earth doped FeGa alloys may be ascribed to the presence of nanoheterogeneties in the samples. The study of order-disorder phase transitions in

$\text{Fe}_{81}\text{Ga}_{19}$  alloys doped with trace amounts ( $\leq 0,2$  at.%) of rare earth elements (RE = Dy, Er, Tb, Yb) by neutron diffraction is presented in [29]. Slow heating and subsequent cooling of the alloys (at a rate of  $\pm 2$  K/min) leads to the formation of  $\text{D0}_3$  phase clusters with sizes in the range of 200 – 300 Å in a matrix of disordered A2 phase. The size and volume fraction of the clusters ( $\approx 0,3$  of the sample volume) depend weakly on the specific composition. A search for structural ordering corresponding to the modified  $\text{D0}_3$  phase ( $\text{D0}_{22}$ ), which was found in a number of electron diffraction studies, did not lead to a positive result.

This study examines the impact of RE-atoms addition on the structural, magnetic and magnetostriction properties of  $\text{Fe}_{80,47}\text{Ga}_{18,75}\text{RE}_{0,78}$  (RE = Tb, Pr, Er) alloys with the  $\text{D0}_3$  phase within the context of density functional theory (DFT) at zero temperature and the Monte Carlo (MC) method at finite temperatures.

## 1. Computational Details

The study of the structural, elastic and magnetostrictive properties of  $\text{Fe}_{80,47}\text{Ga}_{18,75}\text{RE}_{0,78}$  (RE = Tb, Pr, Er) alloys was carried out within the framework of the projector augmented-wave (PAW) method, as implemented in the *ab initio* software package VASP [30,31]. The exchange correlation energy was treated within the generalized gradient approximation in the Perdew, Burke and Ernzerhof parametrization [32]. The electron-ion interactions were described using PAW potentials with the following electronic configurations:  $3p^63d^74s^1$  for Fe,  $3d^{10}4s^24p^1$  for Ga,  $5s^26s^25p^65d^1$  for Pr,  $6s^25p^65d^1$  for Tb, and  $5p^65d^16s^2$  for Er. The plane-wave cut-off energy was set to 650 eV. A Monkhorst-Pack scheme with a  $k$ -point density of  $4 \times 4 \times 4$  was employed to integrate the Brillouin zone in inverse space. The convergence criteria for the total energy was set to  $10^{-6}$  eV/atom.

The geometrical optimization procedure was performed for the  $\text{Fe}_{81,25}\text{Ga}_{18,75}$  and  $\text{Fe}_{80,47}\text{Ga}_{18,75}\text{RE}_{0,78}$  compounds formed on a 128-atom supercell by translating the elementary 16-atom unit cell of cubic symmetry  $\text{D0}_3$  ( $Fm\bar{3}m$  group of symmetry, No 225) in  $2 \times 2 \times 2$  directions. For the binary composition  $\text{Fe}_{81,25}\text{Ga}_{18,75}$  in the 128-atom supercell, 24 Ga atoms were placed at the Wyckoff  $4a$ -positions with coordinates (0, 0, 0). Three types of iron atoms labeled as  $\text{Fe}_1$  (8 atoms),  $\text{Fe}_2$  (32 atoms), and  $\text{Fe}_3$  (64 atoms) were located at the Wyckoff positions  $4a$  (0, 0, 0),  $4b$  (0,5, 0,5, 0,5), and  $8c$  (0,25, 0,25, 0,25), (0,75, 0,75, 0,75), respectively. For ternary alloys, one atom of iron located at Ga-sublattice ( $4a$  positions) was replaced by an atom of RE ( $\text{Fe}_{103}\text{Ga}_{24}\text{RE}_1$ ). Fig. 1 shows the 128-atom supercell of  $\text{Fe}_{103}\text{Ga}_{24}\text{RE}_1$ , representing  $\text{Fe}_{80,47}\text{Ga}_{18,75}\text{RE}_{0,78}$  with the  $\text{D0}_3$  crystal structure. In the upper right corner of Fig. 1, an image of a rare earth element is shown surrounded by iron atoms of the first and second coordination spheres (CS).

The calculation of the tetragonal shear modulus  $C' = (C_{11} - C_{12})/2$  required to estimate the values of the magnetostriction constant was carried out using the strain-stress method [33]. In the elastic stress region  $\sigma = (\sigma_1, \sigma_2, \sigma_3, \sigma_4, \sigma_5, \sigma_6)$  the response of solids to deformation under the application of an external load  $\varepsilon = (\varepsilon_1, \varepsilon_2, \varepsilon_3, \varepsilon_4, \varepsilon_5, \varepsilon_6)$  satisfies the generalized Hooke's law and can be simply represented in the Voigt notation  $\sigma_i = \sum_{j=1}^6 C_{ij}\varepsilon_j$ . The elastic stiffness tensor  $C_{ij}$  was determined using the first-order derivative of the stress-strain curves proposed by Nielsen and Martin [33] with the magnitude of strain  $\varepsilon = \pm 1, 5\%$ .

The magnetostriction coefficient  $\lambda_{001}$  was determined through the magnetocrystalline anisotropy energy ( $E_{\text{MCA}}$ ), the elastic modulus  $C'$ , and the magnetoelastic coefficient  $b_1$

from the following equation [34]:

$$\lambda_{001} = \frac{2dE_{\text{MCA}}/d\varepsilon_z}{3d^2E_{\text{tot}}/d\varepsilon_z^2} = -\frac{b_1}{3C'}, \quad -b_1 = \frac{2}{3V_0} \frac{dE_{\text{MCA}}}{d\varepsilon_z}, \quad (1)$$

$\varepsilon_z$  is the tetragonal strain,  $V_0$  is the cell volume.  $E_{\text{MCA}}$  is the maximum value of the energy difference of the magnetic system when the spins are directed along the different quantization axis. In the present paper, the Fe/RE magnetic moments were rotating from  $z$ -axis to  $[111]$  direction and  $E_{\text{MCA}} = E_{[001]} - E_{[111]}$ . To determine  $E_{[001]}$  and  $E_{[111]}$ , the supercells were deformed from their optimized geometries along the  $z$ -axis in the constant volume mode with the strain value  $\varepsilon_z = \pm 1, 5\%$ . Self-consistent calculations taking into account spin-orbit coupling were performed in the non-collinear VASP mode.

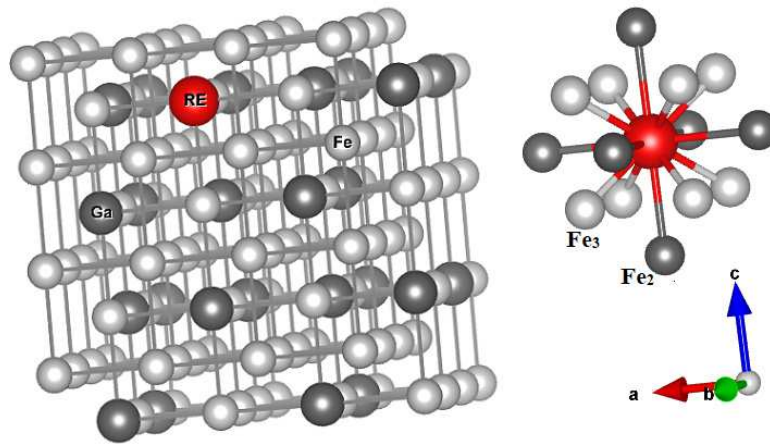


**Fig. 1.** The 128-atom supercell of  $\text{Fe}_{103}\text{Ga}_{24}\text{RE}_1$ , representing  $\text{Fe}_{80,47}\text{Ga}_{18,75}\text{RE}_{0,78}$  with the  $\text{D}_{03}$  crystal structure. The two nearest coordination spheres of the element RE are shown in the upper right corner: the light gray spheres correspond to the first shell, and the dark gray spheres to the second. Iron, labeled  $\text{Fe}_2$  and  $\text{Fe}_3$ , occupies the Wyckoff sites  $4b$  and  $8c$ , respectively. In the binary compound  $\text{Fe}_{81,25}\text{Ga}_{18,75}$ , the element RE corresponds to Ga

Based on the calculated equilibrium lattice constants  $a_0$ , the SPR-KKR [35] package was used to calculate the parameters of the Heisenberg magnetic exchange coupling  $J_{ij}$ . The constants  $J_{ij}$  were calculated using the expression proposed by Liechtenstein et al. All calculations were converged to 0,01 mRy of total energy.

The final step was the Curie temperature estimation with the help of the MC simulations of the three-dimensional Heisenberg model  $\mathcal{H}_{\text{mag}} = -\sum_{ij} J_{ij} \mathbf{S}_i \mathbf{S}_j$ . Here  $\mathbf{S}_i = (S_i^x, S_i^y, S_i^z)$  is a classical magnetic degree of freedom  $|\mathbf{S}_i| = 1$ . Using the calculated  $J_{ij}$ , Fe ( $\mu_{\text{Fe}}$ ) and RE ( $\mu_{\text{RE}}$ ) magnetic moments as input data, the finite-temperature MC simulations of Heisenberg model without magnetic field and anisotropy terms were done. The model lattice with periodic boundary conditions was performed on  $N = 3456$  atoms lattice with periodic boundary conditions using the Metropolis algorithm [36]. The  $\text{D}_{03}$  structure was a  $6 \times 6 \times 6$  array of 16-atoms unit cells. As time unit, we used on MC step consisting of  $N$  attempts to change the spin variables. The total number of MC steps per the temperature step was  $10^6$ . The Curie temperature was estimated from the magnetization-temperature curves  $M(T)$  by plotting the linear intersection of the function  $M^{1/\beta}$  with the temperature axis. Here  $\beta = 0,365$  is the critical index for the three-

dimensional Heisenberg model. The listed calculation stages are presented in more detail in our previous articles [37–42].

## 2. Results and Discussions

### 2.1. Structural Properties

At the first stage of the study, the influence of RE elements on the structural properties of  $\text{Fe}_{81,25}\text{Ga}_{18,75}$  alloys was evaluated. Fig. 2 (a) shows the calculated values of the atomic volume  $V_a = V_0/N$  ( $N = 16$  for  $D0_3$  structure) and elastic moduli  $C'$  depending on the number of  $4f$ -electrons. As can be seen from Fig. 2 (a), the addition of RE elements increases the cell volume per atom by  $\approx 1\%$ . This result is expected due to the significantly larger atomic radius of Pr (1,82 Å), Tb (1,77 Å) and Er (1,76 Å) than that of Fe (1,26 Å) and Ga (1,35 Å). From the lattice parameters along different directions shown in Fig. 2 (a), it is evident that replacing one Fe atom with a RE results in a slight degree of tetragonality ( $a/c < 0,0001$ ). The addition of RE atoms to the  $(\text{Fe}_{83}\text{Ga}_{17})_{100-x}\text{RE}_x$  [26, 28, 43] alloy experimentally confirms the fact of an increase in the lattice parameter. The difference in atomic dimensions leads to low solid solubility of RE in the bcc FeGa matrix, and thus, RE exists mostly in the precipitates [26]. X-ray diffraction data of  $(\text{Fe}_{83}\text{Ga}_{17})_{100-x}\text{Er}_x$  alloys indicates the presence of a single phase having the bcc crystal structure for all samples of composition  $x < 0,6$  (lattice parameter was found  $a = 2,905 \pm 0,005$  Å). In the case of  $(\text{Fe}_{83}\text{Ga}_{17})_{99,94}\text{Pr}_{0,6}$ , the lattice constant of A2 phase was found to be  $\approx 2,904$  Å [43], which is closer to  $(\text{Fe}_{83}\text{Ga}_{17})_{99,94}\text{Tb}_{0,6}$  ( $a = 2,9036$  Å) [28].

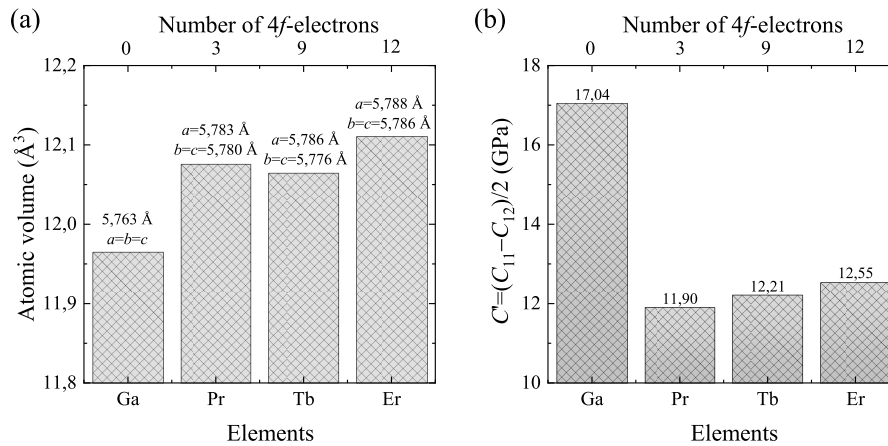


**Fig. 2.** The calculated (a) atomic volume  $V_a = V_0/N$ , and (b) shear modulus  $C'$  for  $\text{Fe}_{81,25}\text{Ga}_{18,75}$ , and  $\text{Fe}_{80,47}\text{Ga}_{18,75}\text{RE}_{0,78}$  alloys with  $D0_3$  structure depending on the number of  $4f$ -electrons.  $a$ ,  $b$  and  $c$  corresponds to the length of vectors along axis  $x$ ,  $y$  and  $z$

Calculation of elastic moduli showed that in the  $D0_3$  phase, the addition of a rare earth metal atom leads to significant softening  $C'$  (see Fig. 2 (b)). In this case, the  $\text{Fe}_{80,47}\text{Ga}_{18,75}\text{Er}_{0,78}$  alloy has the largest value  $C' = 12,55$  GPa, which is due to the smaller atomic radius of Er compared to Pr and Tb. It is likely that a large number of  $4f$  valence electrons and aspherical charge cloud distributions observed in Er atoms lead to enhanced magnetic anisotropy due to crystalline electric field effects.

## 2.2. Magnetostrictive Properties

Recently, many studies have focused on the effects of trace doping with rare earth elements, which have a large number of  $4f$  valence electrons, a non-spherical charge cloud distribution, and strong magnetocrystalline anisotropy between orbitals and spins [43]. It was found that the magnetostriction of Fe–Ga alloys can be enhanced by introducing Tb, Dy, or other rare earth elements. The enhancement of magnetic anisotropy is attributed to the preferential grain orientation and tetragonal distortion induced by the solid solution of rare earth atoms [43]. Fig. 3 (a) shows the calculated magnetocrystalline anisotropy energy  $E_{MCA}$  as a function of tetragonal distortion  $\varepsilon$  for  $\text{Fe}_{81,25}\text{Ga}_{18,75}$  and  $\text{Fe}_{80,47}\text{Ga}_{18,75}\text{RE}_{0,78}$  alloys in  $\text{D}_{03}$  structure. The magnetocrystalline anisotropy energy was defined as the energy difference between magnetization along the direction of uniaxial stress and its perpendicular  $E_{MCA} = E_{[001]} - E_{[111]}$ . The  $E_{MCA}(\varepsilon)$  deformation dependence shows linear behavior with a positive slope in the binary compound. Addition of RE atoms changes the slope to negative. This fact indicates that, compared to  $\text{Fe}_{81,25}\text{Ga}_{18,75}$ , the  $[001]$  direction is not the most stable spin orientation for systems with  $\text{Fe}_{80,47}\text{Ga}_{18,75}\text{RE}_{0,78}$ .

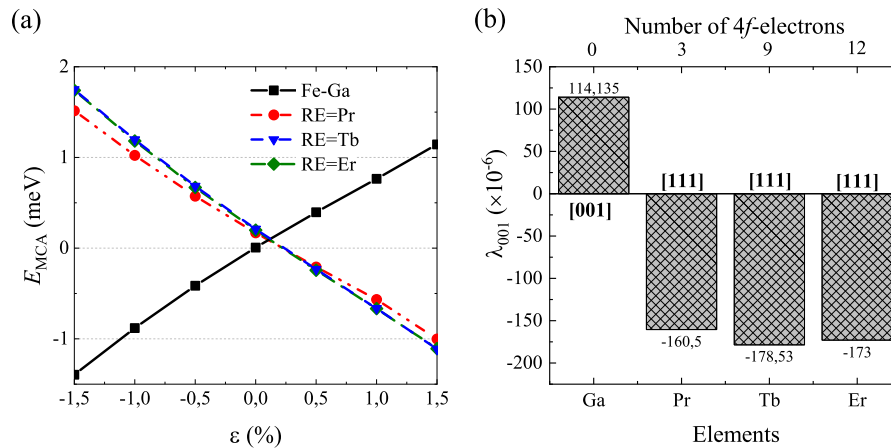


**Fig. 3.** (a) Calculated magnetocrystalline anisotropy energy  $E_{MCA}$  as a function of tetragonal distortion  $\varepsilon$  and (b) tetragonal magnetostriction coefficient  $\lambda_{001}$  for  $\text{Fe}_{81,25}\text{Ga}_{18,75}$  and  $\text{Fe}_{80,47}\text{Ga}_{18,75}\text{RE}_{0,78}$  alloys in  $\text{D}_{03}$ . The most stable directions of orientation of magnetic moments are indicated in square brackets

Fig. 3 (b) shows the constants  $\lambda_{001}$  calculated according to (1). Replacing one Fe atom with a RE atom increases the magnetostriction value, while in the  $\text{Fe}_{80,47}\text{Ga}_{18,75}\text{Tb}_{0,78}$  composition the absolute value of  $\lambda_{001} \approx -179 \times 10^{-6}$  is the largest. In our case, the effect of 0,78 at.% terbium on magnetostriction is 19% in  $\text{D}_{03}$ . The calculation of  $\lambda_{001}$  performed using the DFT in the A2 [44] structure for the  $\text{Fe}_{79,69}\text{Ga}_{19,53}\text{Tb}_{0,78}$  and  $\text{Fe}_{77,78}\text{Ga}_{20,37}\text{Tb}_{1,85}$  alloys showed an increase in magnetostriction by 68% and 59%, respectively, relative to the  $\text{Fe}_{81,48}\text{Ga}_{18,52}$  alloy.

In [24], for  $\text{Fe}_{83}\text{Ga}_{17}\text{M}_{0,2}$  (where M are RE dopants from La to Lu), the dependence of the transverse magnetostriction on the number of  $4f$  electrons was constructed. The biggest excess magnetostriction was found for Ce, Pr, Tb, and Dy, the atoms with the largest negative quadrupole moments. The calculation value of  $\lambda_{001}$  in  $\text{Fe}_{80,47}\text{Ga}_{18,75}\text{Pr}_{0,78}$  is the smallest among alloys with RE atoms. Experimental work shows that rare earth elements have low solubility in the Fe–Ga solid solution and in most cases the addition of

a small amount of  $\approx 0,1$  at.% leads to formation of secondary phases of lower symmetry in the bcc matrix [22, 23, 25–28]. Thus, it can be concluded that the possible increase in magnetostriction in Fe–Ga–RE alloys near the first magnetostriction peak is due to an increase in anisotropy both in the bcc matrix itself and in inclusions.

### 2.3. Magnetic Exchange Constants and Curie Temperature

Analysis of the calculated magnetic moments given in Table for  $\text{Fe}_{81,25}\text{Ga}_{18,75}$  and  $\text{Fe}_{80,47}\text{Ga}_{18,75}\text{RE}_{0,78}$  alloys shows that replacing one Fe atom with RE has no significant effect. Ga, as well as RE atoms, align antiferromagnetically with Fe, with magnetic moments of  $\mu_{\text{Ga}} = -0,11\mu_{\text{B}}/\text{atom}$  and  $\mu_{\text{RE}} = -0,28 \div -0,55\mu_{\text{B}}/\text{atom}$ , and are associated primarily with the  $p$ - and  $d$ - orbitals, respectively. The atomic radius of Er is smaller than that of Pr and Tb, resulting in Fe<sub>3</sub> atoms in first CS of Er having a higher magnetic moment than the same atoms in  $\text{Fe}_{80,47}\text{Ga}_{18,75}(\text{Pr},\text{Tb})_{0,78}$  alloys.

**Table**

Calculated values of the total magnetic moment  $\mu_{\text{tot}}$  ( $\mu_{\text{B}}/\text{atom}$ ), the average magnetic moment per Fe atom  $\bar{\mu}_{\text{Fe}}$  ( $\mu_{\text{B}}/\text{atom}$ ) and partial magnetic moments of three types of Fe atoms  $\mu_{\text{Fe}_{1,2,3}}$ ,  $\mu_{\text{Ga}}$  and  $\mu_{\text{RE}}$  ( $\mu_{\text{B}}/\text{atom}$ ) for  $\text{Fe}_{81,25}\text{Ga}_{18,75}$  and  $\text{Fe}_{80,47}\text{Ga}_{18,75}\text{RE}_{0,78}$  alloys in  $\text{D0}_3$ . The iron atoms labeled as Fe<sub>1</sub>, Fe<sub>2</sub>, and Fe<sub>3</sub> are located at the Wyckoff positions 4a (0, 0, 0), 4b (0,5, 0,5, 0,5), and 8c (0,25, 0,25, 0,25), (0,75, 0,75, 0,75), respectively

Alloy	$\mu_{\text{tot}}$	$\bar{\mu}_{\text{Fe}}$	$\mu_{\text{Fe}_1}$	$\mu_{\text{Fe}_2}$	$\mu_{\text{Fe}_3}$	$\mu_{\text{Ga}}$	$\mu_{\text{RE}}$
$\text{Fe}_{81,25}\text{Ga}_{18,75}$	1,87	2,33	2,51	2,44	2,25	-0,12	—
$\text{Fe}_{80,47}\text{Ga}_{18,75}\text{Pr}_{0,78}$	1,84	2,32	2,50	2,45	2,23	-0,11	-0,28
$\text{Fe}_{80,47}\text{Ga}_{18,75}\text{Tb}_{0,78}$	1,83	2,32	2,50	2,44	2,23	-0,11	-0,46
$\text{Fe}_{80,47}\text{Ga}_{18,75}\text{Er}_{0,78}$	1,88	2,37	2,54	2,46	2,31	-0,11	-0,55

For all compounds the magnetic exchange coupling parameters  $J_{ij}$  were calculated using the equilibrium lattice parameters and the SPR-KKR package by employing coherent potential approximations. The FM state of  $\text{D0}_3$  structure was considered for  $\text{Fe}_{81,25}\text{Ga}_{18,75}$ , and  $\text{Fe}_{80,47}\text{Ga}_{18,75}\text{RE}_{0,78}$  (RE = Tb, Pr, Er) alloys. Figs. 4 (a)–(c) show the dependence of  $J_{ij}$  on the distance  $d/a$  between atoms  $i$  and  $j$  for the first three coordinate spheres.

The magnetic exchange parameters demonstrate the oscillatory behavior and decay with the interatomic distance for all compounds under consideration. Exchange interactions  $J_{ij}^{\text{Ga-Fe/RE}}$  are small and are not included in the consideration. As it shown in earlier studies of  $J_{ij}$  in Fe-based alloys [40–42], the main contribution to the exchange interaction in  $\text{D0}_3$  structure is made by Fe atoms located on different sublattices. In the case of the  $\text{Fe}_{81,25}\text{Ga}_{18,75}$  alloy (see Fig. 4 (a)), the exchange interactions are about 24 and 22.5 meV between Fe<sub>3</sub>-Fe<sub>2</sub> and Fe<sub>3</sub>-Fe<sub>1</sub>, respectively. The addition of Pr and Tb does not affect the above interactions between iron atoms. In the case of Er,  $J_{ij}^{\text{Fe}_3\text{-Fe}_1}$  drastically decreases from 22.5 meV to  $\approx 1$  meV. Such a significant change in magnitude may be the result of exchange interaction between Fe and Er atoms. Fig. 4 (c) shows the values of exchange interactions of RE atoms with Fe atoms located on different sublattices. The Er-Fe<sub>3</sub> and Er-Fe<sub>2</sub> interaction in the first and second coordination spheres (see for detail Fig. 1)  $J_{ij} \approx -3$  meV that indicates antiferromagnetic interactions.

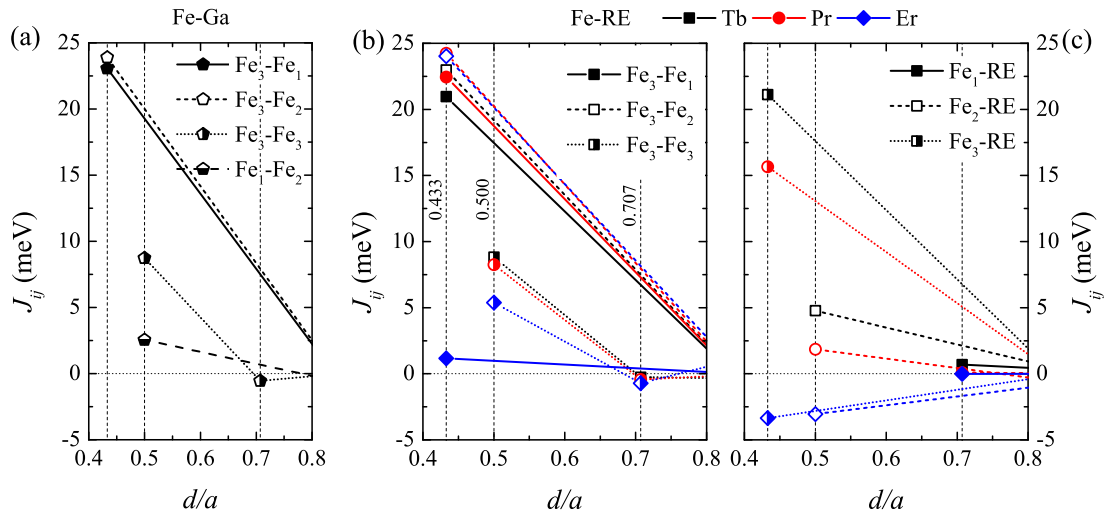


**Fig. 4.** Calculated exchange coupling parameters  $J_{ij}$  as a function of distance ( $d/a$ ) between atoms  $i$  and  $j$  for (a)  $\text{Fe}_{81,25}\text{Ga}_{18,75}$ , and (b, c)  $\text{Fe}_{80,47}\text{Ga}_{18,75}\text{RE}_{0,78}$  ( $\text{RE} = \text{Tb}, \text{Pr}, \text{Er}$ ) alloys. The vertical dotted lines indicate the distance of the first three coordinate spheres  $d/a = \sqrt{3}/4, 1/2, \sqrt{2}/2$

The constants of magnetic exchange interactions and magnetic moments obtained from *ab initio* calculations were used further as input parameters in Heisenberg model to simulate the temperature dependencies of magnetization by MC approach.

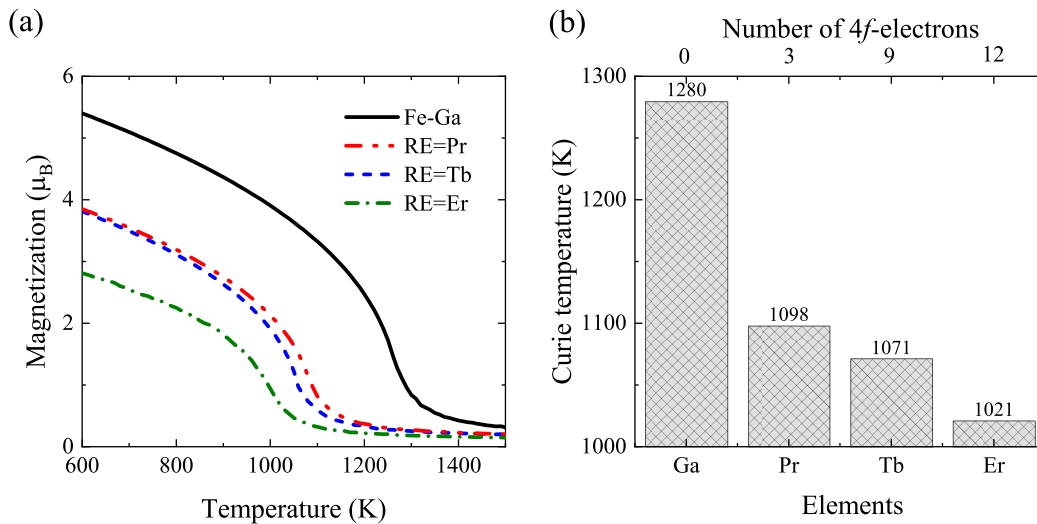


**Fig. 5.** (a) Theoretical temperature dependence of magnetization and (b) Curie temperature of  $\text{Fe}_{81,25}\text{Ga}_{18,75}$ , and  $\text{Fe}_{80,47}\text{Ga}_{18,75}\text{RE}_{0,78}$  alloys

The constants of magnetic exchange interactions and magnetic moments obtained from *ab initio* calculations were further used as input parameters for modeling the temperature dependence of magnetization ( $M$ ). Fig. 5 (a) shows the curves of the  $M(T)$  dependence of  $\text{Fe}_{81,25}\text{Ga}_{18,75}$  and  $\text{Fe}_{80,47}\text{Ga}_{18,75}\text{RE}_{0,78}$  alloys with the  $\text{D0}_3$  structure in the temperature range from 600 to 1500 K using MC modeling of the classical three-dimensional Heisenberg model, performed in zero magnetic fields. The  $M(T)$  curves of compounds with RE

atoms have lower magnetization, indicating that the magnetic interactions weaken upon introduction of RE atoms, in particular, the Fe-RE-Fe interactions remain weaker than Fe-Fe interactions under thermal perturbations. This behavior is confirmed by experimental results. In the work [43], a decrease in the saturation magnetization in the alloy  $(\text{Fe}_{83}\text{Ga}_{17})_{100-x}\text{Pr}_x$  ( $x = 0 \div 1, 0$  at.%) was shown with increasing Pr concentration. Thus, REs contribute to the local paramagnetic ordering in  $\text{Fe}_{81,25}\text{Ga}_{18,75}$  rather than to the strengthening of ferromagnetic interactions.

This decrease in the strength of ferromagnetic interactions leads to a decrease in the Curie temperature  $T_C$ , shown in Fig. 5 (b). A directly proportional dependence of  $T_C$  on the number of electrons in the  $4f$ -orbital can be traced: the more  $f$ -electrons, the lower the Curie temperature. In the  $\text{Fe}_{80,47}\text{Ga}_{18,75}\text{Er}_{0,78}$  alloy,  $T_C$  is 20% lower compared to  $\text{Fe}_{81,25}\text{Ga}_{18,75}$ .

## Conclusion

The present paper reports on the results of *ab initio* calculations obtained by the DFT method at zero temperature and the MC method at finite temperatures in various compositions with the  $\text{D0}_3$  structure. In particular, the results related to the structural and magnetic properties of  $\text{Fe}_{81,25}\text{Ga}_{18,75}$  and  $\text{Fe}_{80,47}\text{Ga}_{18,75}\text{RE}_{0,78}$  (RE = Pr, Tb, Er) alloys are reported. The equilibrium lattice parameter increases with the replacement of the Fe atom by a RE. The presence of RE atoms in the lattice leads to a slight deviation of cubic symmetry to tetragonal. All the compounds considered are mechanically stable, and the addition of RE elements leads to a softening of the shear moduli  $C'$ . The largest value of tetragonal magnetostriction  $\lambda_{001} \approx -179 \times 10^{-6}$  is observed for  $\text{Fe}_{80,47}\text{Ga}_{18,75}\text{Tb}_{0,78}$ , and the effect of 0,78 at.% terbium on magnetostriction is 19% compared to  $\text{Fe}_{81,25}\text{Ga}_{18,75}$ . The addition of rare earth elements leads to a decrease in the Curie temperature, the lowest temperature being found in the  $\text{Fe}_{80,47}\text{Ga}_{18,75}\text{Er}_{0,78}$  alloy. This behavior is due to the presence of antiferromagnetic exchange interactions between Er and Fe atoms in the first and second coordination spheres.

**Acknowledgments.** *This study was supported by the Russian Science Foundation, project no. 24-22-20086, <https://rscf.ru/project/24-22-20086/>.*

## References

1. Clark A.E. Magnetostrictive Rare Earth-Fe<sub>2</sub> Compounds. *Handbook of Ferromagnetic Materials*, 1980, vol. 1, pp. 531–589. DOI: 10.1016/S1574-9304(05)80122-1
2. Engdahl G., Mayergoyz I.D. *Handbook of Giant Magnetostrictive Materials*. San Diego, Academic Press, 2000. DOI: 10.1016/B978-0-12-238640-4.X5014-1
3. Clark A.E., Wun-Fogle M., Restorff J.B., Lograsso T.A. Magnetostrictive Properties of Galfenol Alloys Under Compressive Stress. *Materials Transactions*, 2002, vol. 43, no. 5, pp. 881–886. DOI: 10.2320/matertrans.43.881
4. Kellogg R.A., Flatau A.B., Clark A.E. Wun-Fogle M., Lograsso T.A. Temperature and Stress Dependencies of the Magnetic and Magnetostrictive Properties of  $\text{Fe}_{0,81}\text{Ga}_{0,19}$ . *Journal of Applied Physics*, 2002, vol. 91, pp. 7821–7823. DOI: 10.1063/1.1452216

5. Kellogg R.A., Flatau A.B., Clark A.E., Wun-Fogle M., Lograsso T.A. Texture and Grain Morphology Dependencies of Saturation Magnetostriction in Rolled Polycrystalline Fe<sub>83</sub>Ga<sub>17</sub>. *Journal of Applied Physics*, 2003, vol. 93, no. 10, pp. 8495–8497. DOI: 10.1063/1.1540062
6. Atulasimha J., Flatau A.B. A Review of Magnetostrictive Iron–Gallium Alloys. *Smart Materials and Structures*, 2011, vol. 20, no. 4, article ID: 043001, 15 p. DOI: 10.1088/0964-1726/20/4/043001
7. Xing Qingsong, Du Yingzhou, McQueeney R.J., Lograsso T.A. Structural Investigations of Fe–Ga Alloys: Phase Relations and Magnetostrictive Behavior. *Acta Materialia*, 2008, vol. 56, no. 16, pp. 4536–4546. DOI: 10.1016/j.actamat.2008.05.011
8. Ikeda O., Kainuma R., Ohnuma I., Fukamichi K., Ishida K. Phase Equilibria and Stability of Ordered BCC Phases in the Fe-Rich Portion of the Fe–Ga System. *Journal of Alloys and Compounds*, 2002, vol. 347, no. 9, pp. 198–205. DOI: 10.1016/S0925-8388(02)00791-0
9. Zhang Jingjing, Ma Tianyu, Yan Mi. Anomalous Phase Transformation in Magnetostrictive Fe<sub>81</sub>Ga<sub>19</sub> Alloy. *Journal of Magnetism and Magnetic Materials*, 2010, vol. 322, no. 19, pp. 2882–2887. DOI: 10.1016/j.jmmm.2010.04.045
10. Golovin I.S., Balagurov A.M., Bobrikov I.A., Sumnikov S.V., Mohamed A.K. Cooling Rate as a Tool of Tailoring Structure of Fe-(9–33%) Ga Alloys. *Intermetallics*, 2019, vol. 114, article ID: 106610, 5 p. DOI: 10.1016/j.intermet.2019.106610
11. Golovin I.S., Palacheva V.V., Mohamed A.K., Balagurov A.M. Structure and Properties of Fe–Ga Alloys as Promising Materials for Electronics. *Physics of Metals and Metallography*, 2020, vol. 121, no. 9, pp. 851–893. DOI: 10.1134/S0031918X20090057
12. Restorff J.B., Wun-Fogle M., Hathaway K.B., Clark A.E., Lograsso T.A., Petculescu G. Tetragonal Magnetostriction and Magnetoelastic Coupling in Fe–Al, Fe–Ga, Fe–Ge, Fe–Si, Fe–Ga–Al, and Fe–Ga–Ge Alloys. *Journal of Applied Physics*, 2012, vol. 111, no. 2, article ID: 023905, 12 p. DOI: 10.1063/1.3674318
13. Lograsso T.A., Summers E.M. Detection and Quantification of D03 Chemical Order in Fe–Ga Alloys using High Resolution X-ray Diffraction. *Materials Science and Engineering: A*, 2006, vol. 416, no. 1–2, pp. 240–245. DOI: 10.1016/j.msea.2005.10.035
14. Cao Hu, Bai Feiming, Li Jiefang, Viehland D.D., Lograsso Th.A., Gehring P.M. Structural Studies of Decomposition in Fe–x at.% Ga Alloys. *Journal of Alloys and Compounds*, 2008, vol. 465, no. 1–2, pp. 244–249. DOI: 10.1016/j.jallcom.2007.10.080
15. Clark A.E., Hathaway K.B., Wun-Fogle M., Restorff J.B., Lograsso T.A., Keppens V.M., Petculescu G., Taylor R.A. Extraordinary Magnetoelasticity and Lattice Softening in BCC Fe–Ga Alloys. *Journal of Applied Physics*, 2003, vol. 93, pp. 8621–8623. DOI: 10.1063/1.1540130
16. Wuttig M., Dai Liyang, Cullen J. Elasticity and Magnetoelasticity of Fe–Ga Solid Solutions. *Applied Physics Letters*, 2002, vol. 80, no. 7, pp. 1135–1137. DOI: 10.1063/1.1450045
17. Lograsso T.A., Ross A.R., Schlagel D.L., Clark A.E., Wun-Fogle M. Structural Transformations in Quenched Fe–Ga Alloys. *Journal of Alloys and Compounds*, 2003, vol. 350, no. 1–2, pp. 95–101. DOI: 10.1016/S0925-8388(02)00933-7
18. Ruffoni M.P., Pascarelli S., Grössinger R., Turtelli Sato R., Bormio-Nunes C., Pettifer R.F. Direct Measurement of Intrinsic Atomic Scale Magnetostriction. *Physical Review Letters*, 2008, vol. 101, no. 14, article ID: 147202, 4 p. DOI: 10.1103/PhysRevLett.101.147202
19. Bhattacharyya S., Jinschek J.R., Khachatryan A., Cao Hu, Li Jiefang, Viehland D. Nanodispersed DO<sub>3</sub>– Phase Nanostructures Observed in Magnetostrictive Fe-19% Ga Galfenol Alloys. *Physical Review B–Condensed Matter and Materials Physics*, 2008, vol. 77, no. 10, article ID: 104107, 6 p. DOI: 10.1103/PhysRevB.77.104107

20. Khachatryan A.G., Viehland D. Structurally Heterogeneous Model of Extrinsic Magnetostriction for Fe–Ga and Similar Magnetic Alloys: Part II. Giant Magnetostriction and Elastic Softening. *Metallurgical and Materials Transactions A*, 2007, vol. 38, pp. 2317–2328. DOI: 10.1007/s11661-007-9252-0
21. Keyu Yan, Yichen Xu, Jiejue Niu, Yuye Wu, Yue Li, Gault B., Shiteng Zhao, Xiaoxiao Wang, Yunquan Li, Jingmin Wang, Skokov K.P., Gutfleisch O., Haichen Wu, Daqiang Jiang, Yangkun He, Chengbao Jiang. Unraveling the Origin of Local Chemical Ordering in Fe-Based Solid-Solutions. *Acta Materialia*, 2024, vol. 264, article ID: 119583. DOI: 10.1016/j.actamat.2023.119583
22. Wei Wu, Jinghua Liu, Chengbao Jiang. Tb Solid Solution and Enhanced Magnetostriction in Fe<sub>83</sub>Ga<sub>17</sub> Alloys. *Journal of Alloys and Compounds*, 2015, vol. 622, pp. 379–383. DOI: 10.1016/j.jallcom.2014.09.151
23. Jiang Liping, Yang Jiandong, Hao Hongbo, Zhang Guangrui, Wu Shuangxia, Chen Yajie, Obi Ogheneyunume, Fitchorov T., Harris V.G. Giant Enhancement in the Magnetostrictive Effect of FeGa Alloys Doped with Low Levels of Terbium. *Applied Physics Letters*, 2013, vol. 102, no. 22, article ID: 222409, 5 p. DOI: 10.1063/1.4809829
24. He Yangkun, Jiang Chengbao, Wu Wei, Wang Bin, Duan Huiping, Wang Hui, Zhang Tianli, Wang Jingmin, Liu Jinghua, Zhang Zaoli, Stamenov P., Coey J.M.D., Xu Huibin Giant Heterogeneous Magnetostriction in Fe–Ga Alloys: Effect of Trace Element Doping. *Acta Materialia*, 2016, vol. 109, pp. 177–186. DOI: 10.1016/j.actamat.2016.02.056
25. Emdadi A., Palacheva V.V., Cheverikin V.V., Divinski S., Wilde G., Golovin I.S. Structure and Magnetic Properties of Fe–Ga Alloys Doped by Tb. *Journal of Alloys and Compounds* 2018, vol. 758, pp. 214–223. DOI: 10.1016/j.jallcom.2018.05.073
26. Barua R., Taheri P., Chen Yajie, Koblishka-Veneva A., Koblishka M.R., Jiang Liping, Harris V.G. Giant Enhancement of Magnetostrictive Response in Directionally-Solidified Fe<sub>83</sub>Ga<sub>17</sub>Er<sub>x</sub> Compounds. *Materials*, 2018, vol. 11, no. 6, article ID: 1039, 11 p. DOI: 10.3390/ma11061039
27. Jin T., Wang H., Golovin I.S., Jiang Ch. Microstructure Investigation on Magnetostrictive Fe<sub>100-x</sub>Ga<sub>x</sub> and (Fe<sub>100-x</sub>Ga<sub>x</sub>)<sub>99.8</sub>Tb<sub>0.2</sub> Alloys for  $19 \leq x \leq 29$ . *Intermetallics*, 2019, vol. 115, article ID: 106628. DOI: 10.1016/j.intermet.2019.106628
28. Ke Yubin, Wu Hong-Hui, Lan Si, Jiang Hanqiu, Ren Yang, Liu Sinan, Jiang Chengbao. Tuning Magnetostriction of Fe–Ga Alloys via Stress Engineering. *Journal of Alloys and Compounds*, 2020, vol. 822, article ID: 153687, 9 p. DOI: 10.1016/j.jallcom.2020.153687
29. Balagurov A.M., Yerzhanov B., Mukhametuly B., Samoylova N.Yu., Palacheva V.V., Sumnikov S.V., Golovin I.S. Order–Disorder Phase Transitions in Fe<sub>81</sub>Ga<sub>19</sub>–RE Alloys (RE= Dy, Er, Tb, Yb) According to Neutron Diffraction Data. *Physics of Metals and Metallography*, 2024, vol. 125, no. 2, pp. 185–195. DOI: 10.1134/S0031918X2360286X
30. Kresse G., Furthmuller J. Efficient Iterative Schemes for AB Initio Total-Energy Calculations using a Plane-Wave Basis Set. *Physical Review B*, 1996, vol. 54, pp. 11169–11186. DOI: 10.1103/PhysRevB.54.11169
31. Kresse G., Joubert D. From Ultrasoft Pseudopotentials to the Projector Augmented-Wave Method. *Physical Review B*, 1999, vol. 59, pp. 1758–1775. DOI: 10.1103/PhysRevB.59.1758
32. Perdew J., Burke K., Ernzerhof M. Generalized Gradient Approximation Made Simple. *Physical Review Letters*, 1996, vol. 77, no. 18, pp. 3865–3868. DOI: 10.1103/PhysRevLett.77.3865

33. Wang Vei, Xu Nan, Liu Jin-Cheng, Tang Gang, Geng Wen-Tong. VASPKIT: A User-Friendly Interface Facilitating High-Throughput Computing and Analysis using VASP Code. *Computer Physics Communications*, 2021, vol. 267, article ID: 108033, 19 p. DOI: 10.1016/j.cpc.2021.108033
34. Wang Hui, Zhang Yanning, Wu Ruqian, Sun L.Z., Xu Dongsheng, Zhang Zh. Understanding Strong Magnetostriction in  $\text{Fe}_{100-x}\text{Ga}_x$  Alloys. *Scientific Reports*, 2013, vol. 3, no. 1, article ID: 3521, 5 p. DOI: 10.1038/srep03521
35. Ebert H., Koedderitzsch D., Minar J. Calculating Condensed Matter Properties Using the KKR-green's Function Method—Recent Developments and Applications. *Reports on Progress in Physics*, 2011, vol. 4, no. 9, article ID: 096501, 48 p. DOI: 10.1088/0034-4885/74/9/096501
36. Landau D.P., Binder K. *A Guide to Monte Carlo Simulations in Statistical Physics*. Cambridge, Cambridge University Press, 2009. DOI: 10.1017/CBO9780511994944
37. Matyunina M.V., Zagrebin M.A., Sokolovskiy V.V., Buchelnikov V.D. Magnetostriction of  $\text{Fe}_{100-x}\text{Ga}_x$  Alloys from First Principles Calculations. *Journal of Magnetism and Magnetic Materials*, 2019, vol. 476, pp. 120–123. DOI: 10.1016/j.jmmm.2018.12.038
38. Matyunina M.V., Zagrebin M.A., Sokolovskiy V.V., Buchelnikov V.D. Modelling of Rhombohedral Magnetostriction in Fe–Ga Alloys. *Bulletin of the South Ural State University. Series: Mathematical Modelling, Programming and Computer Software*, 2019, vol. 12, no. 2, pp. 158–165. DOI: 10.14529/mmp190214
39. Zagrebin M.A., Matyunina M.V., Koshkin A.B., Sokolovskiy V.V., Buchelnikov V.D. Structural and Magnetic Properties of Fe–Al Alloys: Ab Initio Studies. *Journal of Magnetism and Magnetic Materials*, 2022, vol. 557, pp. 169437. DOI: 10.1016/j.jmmm.2022.169437
40. Zagrebin M.A., Matyunina M.V., Sokolovskiy V.V., Buchelnikov V.D. The Effect of Exchange-Correlation Potentials on Magnetic Properties of Fe-(Ga, Ge, Al) Alloys. *Journal of Physics: Conference Series*, 2019, vol. 1389, no. 1, article ID: 012087, 7 p. DOI: 10.1088/1742-6596/1389/1/012087
41. Matyunina M.V., Zagrebin M.A., Sokolovskiy V.V., Buchelnikov V.D. Magnetic Properties of  $\text{Fe}_{100-x}\text{Ga}_x$ : Ab Initio and Monte Carlo Study. *Journal of Magnetism and Magnetic Materials*, 2019, vol. 470, pp. 118–122. DOI: 10.1016/j.jmmm.2017.11.011
42. Matyunina M.V., Zagrebin M.A., Sokolovskiy V.V., Buchelnikov V.D. Ab Initio Study of Magnetic and Structural Properties of Fe–Ga Alloys. *EPJ Web of Conferences*, 2018, vol. 185, article ID: 04013, 4 p. DOI: 10.1051/epjconf/201818504013
43. Zhao Lijuan, Tian Xiao, Yao Zhanquan, Zhao Xuan, Wang Rui, Hamt O., Jiang Liping, Harris V.G. Enhanced Magnetostrictive Properties of Lightly Pr-Doped  $\text{Fe}_{83}\text{Ga}_{17}$  Alloys. *Journal of Rare Earths*, 2020, vol. 38, no. 3, pp. 257–264. DOI: 10.1016/j.jre.2019.05.005
44. Adelani M.O., Olive-Méndez S.F., Espinosa-Magaña F., Matutes-Aquino J.A., Grijalva-Castillo M.C. Structural, Magnetic and Electronic Properties of Fe–Ga– $\text{Tb}_x$  ( $0 \leq x \leq 1.85$ ) Alloys: Density-Functional Theory Study. *Journal of Alloys and Compounds*, 2021, vol. 857, article ID: 157540, 29 p. DOI: 10.1016/j.jallcom.2020.157540

Received December 6, 2024

**ВЛИЯНИЕ ЛЕГИРОВАНИЯ РЕДКОЗЕМЕЛЬНЫМИ ЭЛЕМЕНТАМИ НА СВОЙСТВА СПЛАВОВ FE-GA: МОДЕЛИРОВАНИЕ АВ INITIO И МОНТЕ-КАРЛО**

*М.В. Матюнина<sup>1</sup>, А.С. Сокол<sup>1</sup>, О.О. Павлухина<sup>1</sup>, М.А. Загребин<sup>1</sup>,  
В.В. Соколовский<sup>1</sup>, В.Д. Бучельников<sup>1</sup>*

<sup>1</sup>Челябинский государственный университет, г. Челябинск, Российская Федерация

В данной работе изучено влияние малой добавки атомов редкоземельных элементов на структурные, магнитные и магнитомеханические свойства сплавов  $\text{Fe}_{80,47}\text{Ga}_{18,75}\text{PЗМ}_{0,78}$  (PЗМ = Tb, Pr, Er) в фазе  $\text{D0}_3$  в рамках теории функционала плотности и метода Монте-Карло. Геометрическая оптимизация кристаллической решетки, выполненная на 128-атомной суперячейке, показала, что один PЗМ атом замещения приводит к увеличению объема на атом ячейки на  $\approx 1\%$ . Показано, что сплавы  $\text{Fe}_{80,47}\text{Ga}_{18,75}\text{PЗМ}_{0,78}$  механически стабильны, однако наблюдается значительное уменьшение  $C'$ . Добавка атомов PЗМ оказывает существенное влияние на магнитную анизотропию сплава и изменяет направление легкой оси с  $[001]$  на  $[111]$  по сравнению с  $\text{Fe}_{81,25}\text{Ga}_{18,75}$ . Наибольшее значение тетрагональной магнитострикции  $\lambda_{001} \approx -179 \times 10^{-6}$  найдено в сплаве  $\text{Fe}_{80,47}\text{Ga}_{18,75}\text{Tb}_{0,78}$ . Расчетное значение температуры Кюри в композициях с содержанием PЗМ меньше на величину  $\approx 200$  К в сравнении с  $\text{Fe}_{81,25}\text{Ga}_{18,75}$  и наименьшее значение найдено в сплаве  $\text{Fe}_{80,47}\text{Ga}_{18,75}\text{Er}_{0,78}$ . Такое поведение обусловлено наличием антиферромагнитных обменных взаимодействий между атомами Er и Fe в первой и второй координационных сферах.

*Ключевые слова:* магнитострикция; сплавы Fe-Ga; теория функционала плотности; редкоземельные элементы.

Мария Викторовна Матюнина, кандидат физико-математических наук, доцент кафедры физики конденсированного состояния, Челябинский государственный университет (г. Челябинск, Российская Федерация), matunins.fam@mail.ru.

Анна Сергеевна Сокол, лаборант-исследователь кафедры физики конденсированного состояния, Челябинский государственный университет (г. Челябинск, Российская Федерация), sokolanna687@mail.ru.

Оксана Олеговна Павлухина, кандидат физико-математических наук, доцент кафедры радиофизики и электроники, Челябинский государственный университет (г. Челябинск, Российская Федерация), pavluchinaoo@mail.ru.

Михаил Александрович Загребин, доктор физико-математических наук, доцент, профессор кафедры радиофизики и электроники, Челябинский государственный университет (г. Челябинск, Российская Федерация), miczag@mail.ru.

Владимир Владимирович Соколовский, доктор физико-математических наук, доцент, профессор кафедры физики конденсированного состояния, Челябинский государственный университет (г. Челябинск, Российская Федерация), vsokolovsky84@mail.ru.

Василий Дмитриевич Бучельников, доктор физико-математических наук, профессор, заведующий кафедрой физики конденсированного состояния, Челябинский государственный университет (г. Челябинск, Российская Федерация), buche@csu.ru.

*Поступила в редакцию 6 декабря 2024 г.*